2022 American Control Conference (ACC)
Atlanta, USA, June 8-10, 2022

Methodology for Accelerated Inter-Cycle Simulations of Li-ion Battery Degradation with Intra-Cycle Resolved Degradation Mechanisms

Sravan Pannala, Valentin Sulzer, Jason B. Siegel, and Anna G. Stefanopoulou

Abstract— **Accurate predictions of degradation and lifetime of lithium-ion batteries are essential for reliability, safety and key to remanufacturing and repurposing. Cycle life is a key performance metric to understand how changes in the cell design or chemistry will impact system cost and durability. Physics-based models can be used to evaluate battery degradation mechanisms, which is useful when the product lifetime is expected to be 10-20 years and experimental validation is infeasible. The complete lifetime simulation can take hours corresponding to thousands of charge and discharge cycles. An adaptive inter-cycle extrapolation algorithm allows us to rapidly simulate the entire lifetime of the battery and enable the use of optimization algorithms to tune model parameters. We demonstrate the efficacy of the proposed parameter tuning approach using the single particle model with two degradation mechanisms, solid electrolyte interphase growth and active material loss due to mechanical failure. The model can explain the observed trends in capacity fade, loss of lithium inventory and individual electrode capacities from both cycling and calendering experiments. The model agrees well with the data in all outputs, even in cases that were withheld from parameter tuning. The accelerated simulations also agree well with full simulations.**

I. Introduction

Lithium-ion batteries are used widely in portable devices and play an increasingly significant role in transportation and grid storage. These batteries degrade when they undergo charging and discharging and also when they are stored (calendaring). The rate of this degradation depends on how the batteries are used and under what conditions. Even if the Lithium-ion chemistry degrades less than other chemistries, when the battery degrades, its internal impedance and individual electrode capacities change, causing a change in its performance. Hence, we need to model these changes to inform the Battery Management Systems (BMS) to operate the battery safely.

In this work, we consider a hybrid approach of modeling battery degradation [1] , where physics-based models of the degradation mechanism include specific parameters tuned to match the experimental data. The parameterized models can then be used for prognostics or evaluation of aging conditions, including solid electrolyte interphase (SEI) growth, lithium plating, or mechanical effects [2], [3].

One of the challenges of using these physics-based models is that the simulations until the battery reaches its end of life can take hours, making parametrizing model parameters to fit experimental data difficult. Speeding up these aging simulations to a human timescale leads to faster and easier parametrization of the models and can enable the physics-based models to be used as an engineering design tool. The coupling of the degradation mechanism is also improved and can result in a better understanding of various degradation models and the complex interactions among them. Few studies exist in literature on tuning degradation model parameters with data [1], [4], [5]. Tuning of degradation model parameters is mostly done manually to reduce the error between simulation and data [1]. Global optimization techniques [5], [6] are also used to tune model parameters using aging data for entire battery lifetime. These algorithms can take a long time to converge if the time to compute the cost function for each iteration is long. Speeding up the time for each iteration using accelerated simulations makes makes automatic tuning of degradation model parameters using aging data and optimization techniques computationally tractable.

In this paper, we simulate mechanical degradation due to stress and SEI growth to emulate both cycle aging and calendar aging of lithium-ion cells. The model, introduced in Section II, consists of a Single Particle Model (SPM) with SEI growth and stress-driven loss of active material (LAM). The time required for lifetime simulation can be significantly reduced using an adaptive inter-cycle extrapolation algorithm. The main contribution of this work is to the apply algorithm developed in [7] for developing a framework to automatically tune model parameters. Experimental data from the University of Michigan Battery Lab (Section III) was used to tune the model, with good agreement between model and data across both cycle and calendar aging even in conditions that were not used for parameter tuning (Section IV). A summary of this process is given in Fig. 1. The battery model used for our simulations is the SPM.

The cycle-to-cycle model evolution, i.e., when the model states feed and are fed by the evolving degradation variables at each cycle, and the accelerated model with the inter-cycle extrapolation is implemented in PyBaMM (Python Battery Mathematical Modelling) [8] which solves physics-based electrochemical DAE models by using state-of-the-art automatic differentiation and numerical solvers. Other simulation software can also be used to implement the proposed scheme.

II. Modeling and Methodology

We first introduce the concept of accelerated simulations, followed by a description of the degradation model and an

S. Pannala, J.B. Siegel, & A.G. Stefanopoulou are with the Department of Mechanical Engineering, University of Michigan, Ann Arbor, MI 48109 {spannala,siegeljb,annastef}@umich.edu

Valentin Sulzer is with the Department of Mechanical Engineering, Carnegie Mellon University vsulzer@andrew.cmu.edu

978-1-6654-5196-3/$31.00 ©2022 AACC

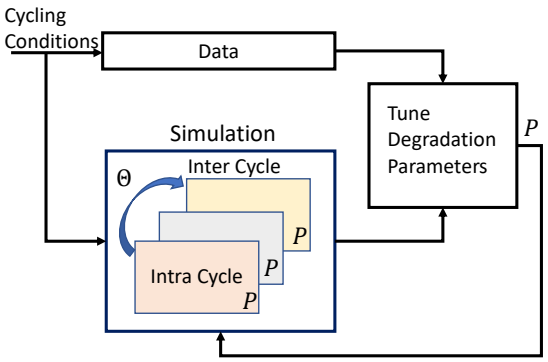

Fig. 1. A summary of the accelerated simulations methodology and tuning of degradation parameters. Here $\boldsymbol{\Theta}$ represents the vector of cycle evolving degradation variables that enables the accelerated inter-cycle simulation and P represents the vector of tunable degradation mechanisms parameters.

automated way to tune model parameters.

A. Accelerated Simulations

Since batteries age over many hundreds of cycles, physics-based simulations of the entire lifetime of a battery can take many minutes or even hours. This is prohibitively slow for iteratively refining the model of the degradation mechanisms and their interaction or tuning the degradation mechanism parameters to match experimental data. To speed this lifetime simulation up, we use an adaptive inter-cycle extrapolation algorithm introduced by Sulzer et al. [7]. This allows simulation of the entire lifetime in just a few seconds, enabling rapid iteration to match experimental data. A brief description of the algorithm is presented in this section, and we refer the reader to [7] for further details.

The adaptive inter-cycle extrapolation algorithm is based on two key ideas: first, since the degradation timescale is slow relative to the cycling timescale, the change in the degradation variables over one cycle can be extrapolated over several cycles (Figure 2); and second, this can be done adaptively for optimal accuracy-efficiency trade-off. We first explain the fixed-step inter-cycle extrapolation algorithm, as introduced for example by Kupper et al. [9] and Vora et al. [10]. At each iteration of this algorithm, we first calculate the amount of degradation over a single cycle by directly simulating the cycle, then linearly extrapolate the amount of degradation over n cycles. The hyper-parameter n must be selected ahead of time to take large enough steps while remaining accurate in non-linear regions, which is difficult to do: different degradation models will have different optimal step sizes.

This difficulty in hyper-parameter selection naturally suggests that the algorithm should be made adaptive, with the extrapolation step size depending on the rate of change of degradation rate. Since the underlying degradation is continuous from cycle to cycle, we can thus write an ODE

$$\frac{\mathrm{d}\boldsymbol{\Theta}}{\mathrm{d}t} = \Delta\boldsymbol{\Theta}, \tag{1}$$

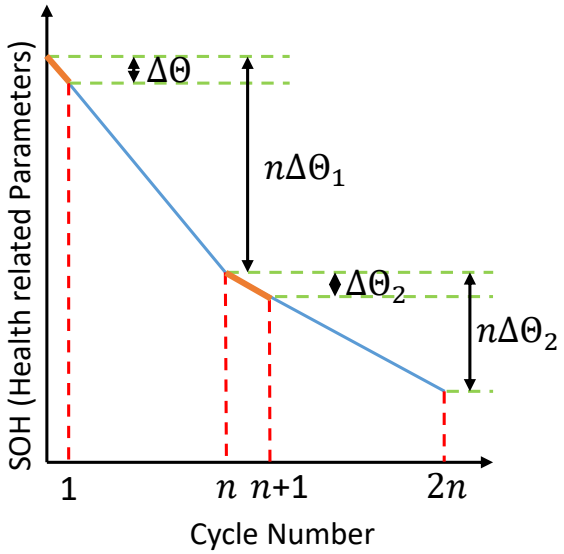

Fig. 2. Inter-cycle extrapolation, from [7]. The change in SOH parameters over one cycle, Δy_1, is assumed to be constant for the next n cycles, resulting in a $n\Delta y_1$ change over n cycles. The change in SOH over the n^{th} cycle is then calculated and extrapolated to the $2n^{\text{th}}$ cycle, etc. Here SOH represents an internal degradation variable of the model, of which there can be several, for example SEI thickness (k_{SEI}) or active material volume fraction in either electrode ($\varepsilon_{\text{s}}^{\pm}$).

where $\boldsymbol{\Theta}$ represents the vector of slowly changing degradation variables. We can then solve this ODE using any adaptive time-stepping algorithm (Runge-Kutta 3(2) [11] in this paper).The extrapolation step size is automatically determined by the adaptive ODE solver. At each timestep in the ODE solver, we must solve a full charge/discharge cycle obtain $\Delta\boldsymbol{\Theta}$. We use PyBaMM [8] to simulate these single cycles.

B. Degradation Mechanism Model

Battery degradation occurs during its lifetime, and its common observed effects are capacity loss, loss of cyclable lithium, and increase in resistance. Several degradation mechanisms have been proposed to explain and model these changes in battery parameters [1]. In our study, we model and simulate battery degradation caused by SEI formation in the negative electrode and mechanical damage in both the positive and negative electrodes. The equations of the degradation mechanisms and the battery and their interactions are summarized in Fig. 3. Further description of the model variables and parameters is given in Table III. The SEI model used is adopted from [2] and the mechanical damage is based on fatigue damage due to cyclic loading of particle stress. The stresses in the particle are computed based on work by [12]. The loss of active material can be correlated to the hydrostatic stress in the electrode particle [1]. The empirical relationship is given by

$$\frac{d\varepsilon}{dt} = \beta_{\text{LAM}} \left(\frac{\sigma_{\text{h,max}} - \sigma_{\text{h,min}}}{\sigma_{\text{yield}}} \right)^{m_{\text{LAM}}}, \tag{2}$$

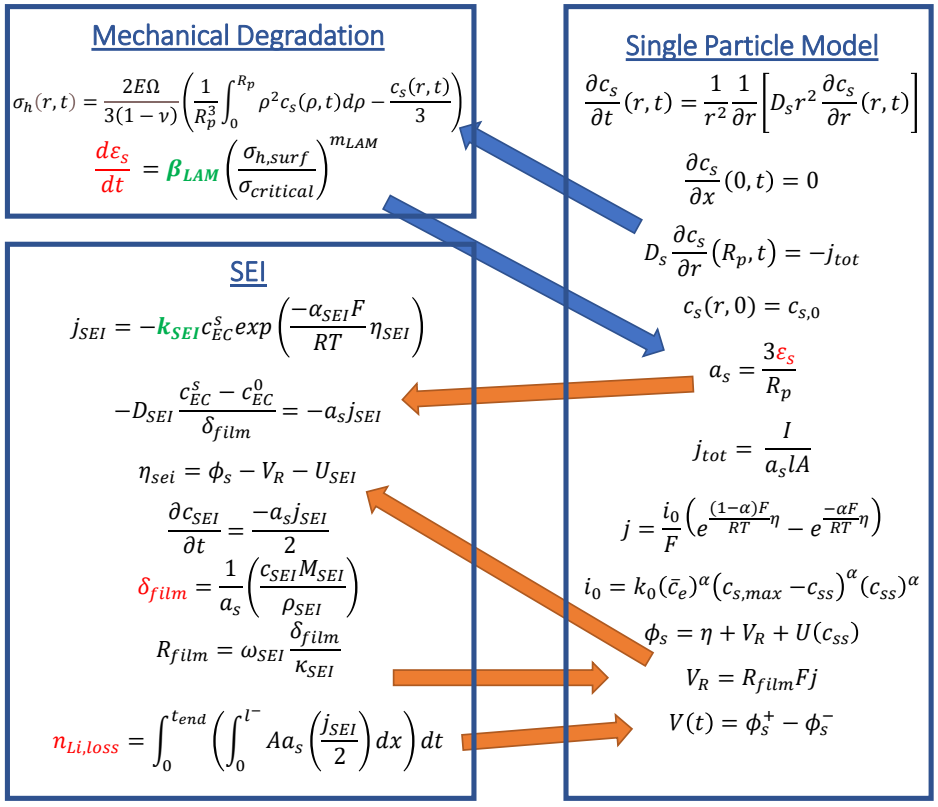

Fig. 3. Interaction between the degradation mechanisms. Further description of the model variables and parameters is given in Table III. The blue lines show the interaction between the mechanical damage model and the battery. The orange lines represent the interaction between the SEI formation model and the battery. Mechanical damage leads to the loss of active material. This loss increases the particle's current density, leading to larger concentration gradients in the particle and thus higher stresses as the battery ages. SEI formation increases battery resistance affecting the overpotentials of reactions in the battery and the terminal voltage. Another consequence of SEI formation is the loss of cyclable lithium.

where $\sigma_{h,max}$ and $\sigma_{h,min}$ are the maximum and minimum particle stresses and the β_{LAM} and m_{LAM} are tuning parameters Assuming maximum particle stress at the surface and minimum stress as zero, Eq. (2) was simplified as:

$$\frac{d\varepsilon}{dt} = \beta_{\text{LAM}}\left(\frac{\sigma_{\text{h,surf}}}{\sigma_{\text{yield}}}\right)^{m_{\text{LAM}}} \tag{3}$$

1) Interactions Between the Degradation Mechanisms: The interactions between degradation mechanisms and with the battery are discussed in this section. First, let's explore mechanical degradation. The hydrostatic stress at the particle's surface is directly proportional to the lithium concentration gradient in the particle. This stress then leads to particle damage resulting in loss of active material (LAM) of the electrode, causing a decrease in the active material ratio ε_{s}, which decreases the active material to surface ratio a_{s}. This in turn, causes an increase in current density, leading to a higher concentration gradient in the particle, resulting in higher particle stress. This decrease in a_{s} also affects the SEI formation reaction as shown in Fig. 3. The main effect of SEI formation is the increase in negative electrode film resistance R_{film} and loss of lithium inventory [LLI] given by $n_{\text{Li,loss}}$. The increase in resistance affects the overpotentials of reactions occurring in the battery, including side reactions like SEI formation. The battery terminal voltage is also affected by this resistance change causing the voltage limits to be reached faster and thus reducing the battery capacity when cycling. The LLI due to SEI formation also causes a change in the stoichiometric limits for positive electrode $[y_0, y_{100}]$ and for negative electrode $[x_0, x_{100}]$ which also results in changes in the voltage output of the battery.

2) Defining the Degradation Variables and Model Parameters: We now describe the vector of degradation variables Θ based on the degradation mechanisms discussed in the previous sections. These are the three state variables for the degradation equations (δ_{SEI}, ε_{s}^-, and ε_{s}^+), plus the total lithium inventory, $n_{\text{Li,s}}$, which is used instead of the particle concentration state variables to track LLI $\left(\text{LLI} = (1 - \frac{n_{\text{Li,s}}}{n_{\text{Li,s,init}}})\right)$ since degradation variables should evolve on the slow degradation timescale [7].

$$\boldsymbol{\Theta} = \left[\delta_{\text{SEI}}, \varepsilon_{\text{s}}^-, \varepsilon_{\text{s}}^+, n_{\text{Li,s}}\right]^T \tag{4}$$

The first variable here is the amount of cyclable lithium in the battery $n_{\text{Li,s}}$ which decreases due to the lithium loss in the battery. The second variable is the thickness of the SEI layer δ_{SEI}, which increases due to the formation of new SEI as the battery ages. The last two variables are active material ratios of the negative and positive electrodes, $[\varepsilon_{\text{s}}^-, \varepsilon_{\text{s}}^+]$ which decreases according to Eq. (3). C_{n} & C_{p} are related to the

$\varepsilon_{\mathrm{s}}^{-}$ and $\varepsilon_{\mathrm{s}}^{+}$ by this equation:

$$C_{\mathrm{p,n}} = \frac{\varepsilon_{\mathrm{s}}^{\pm} A l^{\pm} c_{\mathrm{s,max}}^{\pm} F}{3600} \tag{5}$$

Next, we define the vector of degradation mechanism parameters to be tuned to match the model with data. These are:

$$P = \left[k_{\mathrm{SEI}}, \beta_{\mathrm{LAM}}^{-}, \beta_{\mathrm{LAM}}^{+}\right]^T \tag{6}$$

The description of these parameters and their values used in this paper are given in Table II.

C. Parameter fitting

This section introduces a tuning methodology to fit the degradation mechanism model output to the data. We want to take advantage of the fact that the simulation time for a battery's lifetime takes only a few seconds. Least squares optimization can be used on the simulation output and the data to get the tuned model parameters. However, it is not possible to calculate the derivatives for the optimization in our case. So we utilize derivative-free least squares optimization algorithm DFO-LS [13] which does not require us to provide derivatives for optimization and does not attempt to estimate them internally.

1) Define vector of degradation mechanism parameters P to be tuned for a particular problem.
$$P = \left[p^1, p^2, \ldots, p^{n_1}\right]^T \tag{7}$$
2) Define a vector of data to be fitted against the model outputs.
$$Y = \left[y^1, y^2, \ldots, y^{n_2}\right]^T \tag{8}$$
3) Use values from literature as initial guess.
4) Run DFO-LS to solve least squares optimization problem to estimate degradation mechanism model parameters.

$$\begin{aligned}\hat{P} &= \arg\min_{P} f(x) \\ &= \sum_{j=1}^{n_2} w^j \sum_{i=1}^{m} \left(y_i^j - model^j(x_i, P)\right)^2 \end{aligned} \tag{9}$$

where $model^j(x_i, P)$ is the corresponding model output to the data y^j for the observation point x_i. The number of observation points m refers to the number of performance tests discussed in Section III-B. Appropriate weights w^j are applied to normalize the outputs.

Now, let's define the P and Y vectors for the two degradation mechanisms we are trying to tune parameters for:

1) Calendar Aging: First, we tune the degradation due to SEI formation using the data from the calendar aged cell. In this case, there is no mechanical degradation because there is no cycling of the current in the cell. We want to tune the SEI degradation parameter k_{SEI} to fit the battery capacity C and amount of cyclable lithium n_{Li}, which is related to the loss of lithium inventory (LLI). So, P and Y here are:

$$P = [k_{\mathrm{SEI}}] \tag{10}$$
$$Y = [C, n_{\mathrm{Li}}]^T \tag{11}$$

2) Constant Current Cycling Aging: Next, utilizing parameter k_{SEI} tuned in the previous section for the SEI degradation model, we tune the mechanical degradation model parameters β_{LAM}^{-} and β_{LAM}^{+} to fit the capacity C, and the electrode capacities C_{n} & C_{p}. P and Y here are:

$$P = \left[\beta_{\mathrm{LAM}}^{-}, \beta_{\mathrm{LAM}}^{+}\right] \tag{12}$$
$$Y = [C, C_{\mathrm{n}}, C_{\mathrm{p}}]^T \tag{13}$$

III. Experiments and Data

The degradation experiments were performed on NMC/Graphite energy cells manufactured in a single batch at the University of Michigan Battery Lab (UMBL). Further details of the battery parameters and the experiments can be found in work by Mohtat et al. [14]. The aging process of the cells used in this study is summarized in Section III-A followed by the aging characterization method and eSOH (Electrode State of Health) estimation in Section III-B.

A. Aging Methodology

The cells used in this study were placed in a battery fixture located in a thermal chamber set at 25°C. Then, two different types of aging were performed on the batteries:

1) Calendar Aging: Calendar aging at two different state of charge (SOC) was performed. One cell was fully charged (100% SOC), and the second cell was discharged to 50% SOC before being placed in the fixture. These cells were then calendar aged for 250 days.

2) Constant Current Cycling Aging: Here the batteries were cycled at a constant current for 100% depth of discharge (DOD) and 50% DOD. The cycling is composed of a constant current (CC) charge at C/5 until the battery reaches 4.2 V, followed by constant voltage charging (CV) at 4.2 until the current drops below C/50. Then a CC discharge was performed till the battery reached 3.0 V. For the 50% discharge case, the DOD is with respect to nominal capacity.

B. Performance Testing and eSOH calculation

The above cells were cycled to at least 80% capacity retention, and the characterization tests were performed periodically. These tests include C/20 charge-discharge cycle required for eSOH estimation. The C/20 charge voltage data is used for estimating eSOH parameters by using the voltage fitting method as described in [15]. The eSOH parameters estimated here are capacities of positive and negative electrodes C_{p} and C_{n} and the electrode utilization range/ stoichiometric limits for positive electrode $[y_0, y_{100}]$ and for negative electrode $[x_0, x_{100}]$.

TABLE I
Time for Experiments and Simulations

	Cycling conditions	
	Calendar Aging	C/5 Cycling
Experiment	250 days	150 days
Full Simulations	4 minutes	3 minutes
Accelerated Simulations	17 seconds	10 seconds
Parameter Tuning	3 minutes	4 minutes

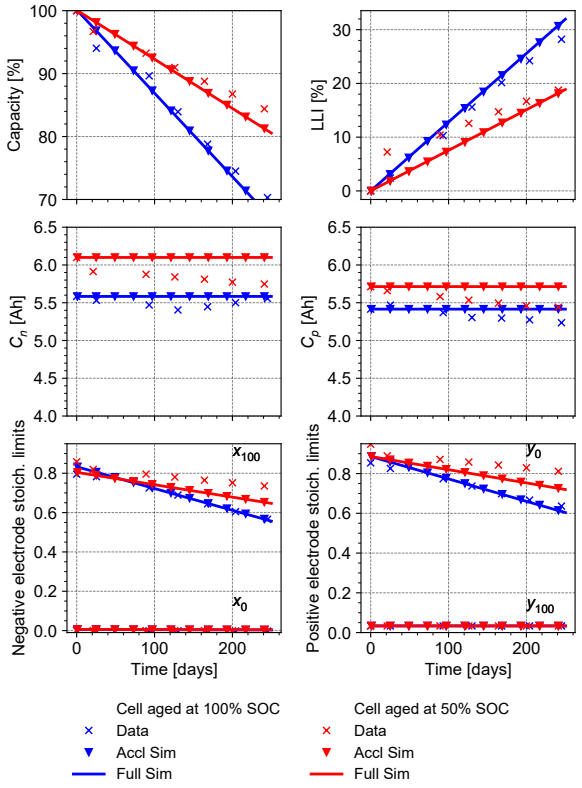

Fig. 4. Calendar aging calculated from data from batteries stored at 100% SOC and 50%. Capacity, LLI, and eSOH parameters are shown here for data, accelerated simulations, and full simulations. Capacity loss due to SEI formation was tuned for the cell stored at 100% (blue). eSOH parameters from the data match well with the simulated results. The model predicts well the capacity loss and eSOH parameters of the cell stored at 50% SOC (red) using the parameters tuned for the cell stored at 100% SOC (blue).

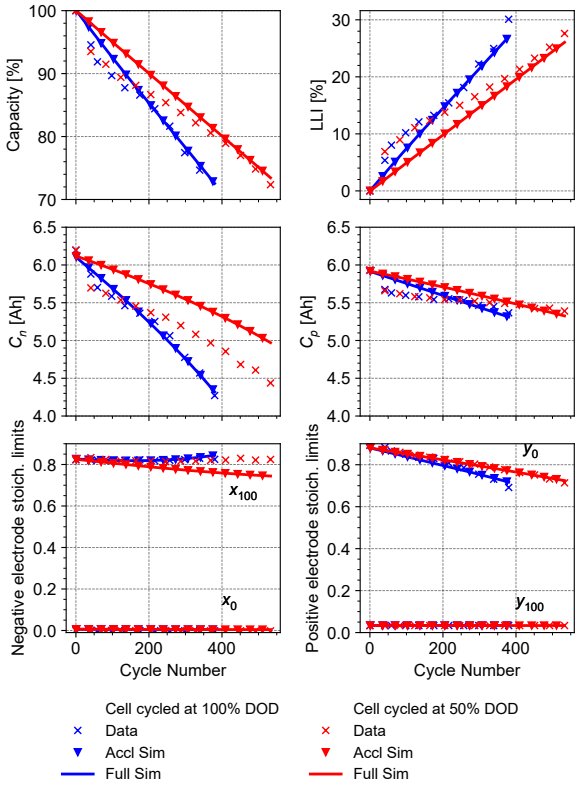

Fig. 5. Cycle aging for cells cycled at C/5 for 100% DOD and 50% DOD. Mechanical degradation parameters $\beta^{\pm}_{\mathrm{LAM}}$ are tuned to match changes in C_{p} and C_{n}. The simulations capture LLI and electrode stoichiometric limits shown in data (blue). Then the model with $\beta^{\pm}_{\mathrm{LAM}}$, k_{SEI} estimated previously is used to predict the degradation in 50% DOD cell (red). The capacity loss in the simulations is found to be a good fit with data. While the simulations capture the trend of changes in LLI and eSOH parameters, there is still a small error compared to data.

IV. Results and Discussion

A. Calendar Aging

The model was simultaneously tuned to match both the calendar and cycle aging data using the methodology given in Section II-C. The identified parameters are shown in Table II. A comparison of the capacity and key eSOH indicators extracted from the model simulation and experimental data are shown in Fig. 4. The accelerated and normal simulations show almost identical results, C_{p} and C_{n} do not change much. The positive and electrode stoichiometric limits are also in good agreement with the data. The simulation time for both accelerated simulations and full simulations is given in Table I where the accelerated simulation results in a 27x speedup. The simulations are performed on a computer with Intel® Core™ i7-8550U CPU Processor with 1.80GHz clock speed.

Fig. 4 also shows the comparison for the calendar aging at 50% SOC. The model captures the capacity loss well but under-predicts the LLI. The eSOH parameters show us that in the simulations there is a faster decrease in the stoichiometric windows of the cells x_{100} and y_0 compared to data. Also, the data shows a small decrease in C_{n} and C_{p} which is not seen in our simulations.

B. Cycling Aging at C/5 at different Depth of Discharge

Next, we perform the simulations for cycling aging at C/5 current. The eSOH and LLI from the simulations are in excellent agreement as shown in Fig. 5. The stoichiometric limits in the simulations also show similar trends to the data.

Now using the parameters tuned in the previous section, which are shown in Table II, we simulate the degradation for the C/5 50% DOD cycling. These results are also shown in Fig. 5. The overall capacity loss seems to be captured well by the simulation, although the LLI is slightly smaller compared to the data. For the eSOH parameters, while we get a good fit for y_0, C_{n} is higher in our simulations, x_{100} decreases while it stays constant in the data, and we miss the initial drop in C_{p} and C_{n}. The lower LLI at the initial

TABLE II
Degradation Parameters used for Accelerated Simulations

Parameter	Meaning	Value
k_{SEI}	SEI kinetic rate constant [m/s]	1.683×10^{-16}
β^{-}_{LAM}	Anode Cracking rate [1/s]	5.803×10^{-5}
β^{+}_{LAM}	Cathode Cracking rate [1/s]	8.357×10^{-6}

part of aging is also because we do not capture the initial drop in electrode capacity.

V. Conclusion

This paper discusses the need for fast aging simulations and applies an adaptive inter-cycle extrapolation algorithm introduced in [7] for developing a framework to automatically tune degradation model parameters. The degradation mechanisms of SEI formation and mechanical damage were introduced, and their interactions and effect on battery parameters were described. First, we tune the SEI degradation parameter to match capacity loss data from a cell calendar aged at 100% SOC and compare the model prediction with data from a cell calendar aged at 50%. The simulations show that the data and prediction of capacity, LLI, and eSOH parameters fit well. Then the mechanical damage model was tuned to fit electrode capacity data from a cell cycled at C/5 for 100% depth of discharge. The simulations show a good fit for capacity, LLI, and electrode stoichiometric limits. Finally, the model with all the degradation parameters identified and fixed was used to predict eSOH parameters of a cell cycled at C/5 for 50% DOD and compared with actual degradation data. The fit of the capacity loss, C_p and y_0 with the data is good, but the fit of the other eSOH parameters is not as good, although the simulations are capturing the correct trend. For all these cases, the accelerated simulations results are in excellent agreement with the normal cycle-resolved simulations. Other degradation conditions will be explored in future work. Accelerated simulations lead to faster parameterization of physics-based degradation models and can enable these models to be used as interactive engineering design and discovery tools.

TABLE III
Description of Model Variables and Parameters

Variable/Parameter	Meaning
$n_{\mathrm{Li,s}}$	Amount of cyclable Li [mol]
δ_{SEI}	Thickness of SEI layer [m]
ε_{s}	Active material ratio
m_{LAM}	LAM exponent
σ_{h}	Hydrostatic stress in the particle [Pa]
E	Young's modulus of the electrode material [Pa]
Ω	Partial molar volume [m^3/mol]
ν	Poisson's ratio
c_{s}	Conc. of Li in electrode [mol/m^3]
ε_{s}	Active material ratio
R_{p}	Radius of particle [m]
$\sigma_{\mathrm{critical}}$	Critical stress of the electrode [Pa]
j_{tot}	Total current density in the electrode [A/m^2]
a_{s}	Surface area to volume ratio [1/m]
l	Length of electrode [m]
A	Area of electrode [m^2]
η	Bulter-Volmer overpotential [V]
i_0	Exchange current density [A/m^2]
k_0	Exchange current density [$\mathrm{A m}^{-2}(\mathrm{m}^3\mathrm{mol})^{-1.5}$]
α	Charge transfer coefficient
c_{e}	Conc. of Li in electrolyte [mol/m^3]
ϕ_s	Potential of electrode [V]
U	Open circuit potential of electrode [V]
V_{R}	Voltage drop across film resistance [V]
j_{SEI}	Current density of SEI formation [A/m^2]
$c^{\mathrm{s}}_{\mathrm{EC}}$	Conc. of solvent in electrolyte [mol/m^3]
α_{SEI}	Charge transfer coefficient of SEI formation
D_{SEI}	SEI layer diffusivity [m^2/s]
η_{SEI}	Overpotential of SEI formation [V]
U_{SEI}	Potential of SEI formation [V]
c_{SEI}	Conc. of SEI layer in electrode [mol/m^3]
M_{SEI}	Molar conc. of SEI layer [mol/m^3]
ρ_{SEI}	Density of SEI layer [kg/m^3]
ω_{SEI}	Volume fraction of SEI in the film
κ_{SEI}	Ionic conductivity of SEI [S/m]

References

[1] J. M. Reniers, G. Mulder, and D. A. Howey, "Review and Performance Comparison of Mechanical-Chemical Degradation Models for Lithium-Ion Batteries," *Journal of The Electrochemical Society*, vol. 166, no. 14, pp. A3189–A3200, 2019.

[2] X. G. Yang, Y. Leng, G. Zhang, S. Ge, and C. Y. Wang, "Modeling of lithium plating induced aging of lithium-ion batteries: Transition from linear to nonlinear aging," *Journal of Power Sources*, vol. 360, pp. 28–40, 2017. [Online]. Available: http://dx.doi.org/10.1016/j.jpowsour.2017.05.110

[3] I. Laresgoiti, S. Käbitz, M. Ecker, and D. U. Sauer, "Modeling mechanical degradation in lithium ion batteries during cycling: Solid electrolyte interphase fracture," *Journal of Power Sources*, vol. 300, pp. 112–122, 2015.

[4] V. Sulzer, P. Mohtat, A. Aitio, S. Lee, Y. T. Yeh, M. U. Khan, J. W. Lee, J. B. Siegel, A. David, and A. G. Stefanopoulou, "The challenge of battery lifetime prediction from field data," *Joule*, pp. 1–20, 2021. [Online]. Available: https://doi.org/10.1016/j.joule.2021.06.005

[5] Y. Gao, X. Zhang, C. Zhu, and B. Guo, "Global Parameter Sensitivity Analysis of Electrochemical Model for Lithium-Ion Batteries Considering Aging," *IEEE/ASME Transactions on Mechatronics*, vol. 26, no. 3, pp. 1283–1294, Jun. 2021. [Online]. Available: https://ieeexplore.ieee.org/document/9384294/

[6] A. Bills, S. Sripad, W. L. Fredericks, M. Guttenberg, D. Charles, E. Frank, and V. Viswanathan, "Universal Battery Performance and Degradation Model for Electric Aircraft," *arXiv:2008.01527 [physics]*, Mar. 2021. [Online]. Available: http://arxiv.org/abs/2008.01527

[7] V. Sulzer, P. Mohtat, S. Pannala, J. B. Siegel, and A. G. Stefanopoulou, "Accelerated Battery Lifetime Simulations Using Adaptive Inter-Cycle Extrapolation Algorithm," *Journal of The Electrochemical Society*, vol. 168, no. 12, p. 120531, Dec. 2021. [Online]. Available: https://iopscience.iop.org/article/10.1149/1945-7111/ac3e48

[8] V. Sulzer, S. Marquis, R. Timms, M. Robinson, and S. J. Chapman, "Python Battery Mathematical Modelling (PyBaMM)," *Journal of Open Research Software*, vol. 9, no. 1, p. 14, 2021.

[9] C. Kupper, B. Weißhar, S. Rißmann, and W. G. Bessler, "End-of-Life Prediction of a Lithium-Ion Battery Cell Based on Mechanistic Aging Models of the Graphite Electrode," *Journal of The Electrochemical Society*, vol. 165, no. 14, pp. A3468–A3480, 2018.

[10] A. P. Vora, X. Jin, V. Hoshing, G. Shaver, S. Varigonda, and W. E. Tyner, "Integrating battery degradation in a cost of ownership framework for hybrid electric vehicle design optimization," *Proceedings of the Institution of Mechanical Engineers, Part D: Journal of Automobile Engineering*, vol. 233, no. 6, pp. 1507–1523, 2019.

[11] P. Bogacki and L. F. Shampine, "A 3 (2) pair of runge-kutta formulas," *Applied Mathematics Letters*, vol. 2, no. 4, pp. 321–325, 1989.

[12] X. Zhang, W. Shyy, and A. Marie Sastry, "Numerical Simulation of Intercalation-Induced Stress in Li-Ion Battery Electrode Particles," *Journal of The Electrochemical Society*, vol. 154, no. 10, p. A910, 2007.

[13] C. Cartis, J. Fiala, B. Marteau, and L. Roberts, "Improving the flexibility and robustness of model-based derivative-free optimization solvers," *ACM Transactions on Mathematical Software*, vol. 45, no. 3, 2019.

[14] P. Mohtat, S. Lee, J. Siegel, and A. Stefanopoulou, "Reversible and irreversible expansion of lithium-ion batteries under a wide range of stress factors," *Journal of The Electrochemical Society*, 2021. [Online]. Available: http://iopscience.iop.org/article/10.1149/1945-7111/ac2d3e

[15] S. Lee, J. B. Siegel, A. G. Stefanopoulou, J.-W. Lee, and T.-K. Lee, "Comparison of individual-electrode state of health estimation methods for lithium ion battery," in *Dynamic Systems and Control Conference*, vol. 51906. American Society of Mechanical Engineers, 2018, p. V002T19A002.